JOURNAL OF THE AMERICAN WATER RESOURCES ASSOCIATION

AMERICAN WATER RESOURCES ASSOCIATION

Trends in Raindrop Kinetic Energy with Modeled Climate Warming in the Lake Tahoe Basin

Jack Lewis and Robert Coats

Research Impact Statement: More precipitation falling as rain and briefer snow cover would increase the kinetic energy of rain falling on snow-free ground, hence may increase surface soil erosion in the Lake Tahoe Basin.

ABSTRACT: Two means by which climate change may increase surface soil erosion in mountainous terrain are: (1) increasing the frequency of extreme rainfall events and (2) decreasing the duration of snow cover on bare soil. We used output from four general circulation models (GCMs) and two greenhouse gas trajectories to produce a suite of hydrologic variables at a daily time-step for historic and projected 21st Century conditions. We statistically disaggregated the daily rainfall to hourly, using hourly rainfall from a network of nine weather stations in the Tahoe Basin, and filtered out rain falling on a snowpack. We applied published equations to convert hourly intensity to raindrop kinetic energy (KE) for each day and grid cell in the Basin, averaged across grid cells, and created time series of total annual and maximum annual hourly kinetic energy (TKE and MKE) on snow-free ground. Using the Generalized Extreme Value distribution, we calculated the significance of long-term trends in KE on snow-free ground, and estimated energy levels for return periods of 2, 20, and 100 years. We then detrended the snowpack data and compared the resulting trends in KE with the trends resulting from changes in both rainfall energy and snowpack under two GCMs. Principal findings include (1) upward trends in MKE, (2) stronger upward trends in TKE; and (3) an effect of increasing rainfall intensities on KE in some cases, and a strong effect of reduced snowpack in all cases examined.

(KEYWORDS: climate change; Lake Tahoe; raindrops; kinetic energy; snow hydrology; extreme values.)

INTRODUCTION

Lake Tahoe is a large ultra-oligotrophic lake lying at an elevation of 1,898 m in the central Sierra on the California-Nevada border (Figure 1). The lake is renowned for its deep azure color and clarity. Due to concerns about progressive eutrophication and loss of clarity, the lake has been studied intensively for a half-century, and has been the focus of major efforts to halt the trends in clarity and trophic status. The loss of clarity has been attributed to input of nitrogen and phosphorus from atmospheric deposition and watershed disturbance, and to input of fine (<20 μ) sediment, much of it originating from disturbed soils in developed areas (Roberts and Reuter 2007).

While California's climate will almost certainly continue warming in future decades, climate models diverge with respect to annual precipitation. Pierce et al. (2013) examined 25 downscaled general circulation model (GCM) projections through the 2060s and found that 21 predicted a decrease in the frequency of precipitation (wet days per year) and 16 predicted an increase in its intensity, with 12 models showing drier annual conditions and 13 showing wetter.

Paper No. JAWRA-19-0049-P of the *Journal of the American Water Resources Association* (JAWRA). Received March 26, 2019; accepted February 6, 2020.

Pacific Southwest Research Station (Lewis [retired]), USDA Forest Service, Arcata, California, USA; and Tahoe Environmental Research Center (Coats), Incline Village, Nevada, USA (Correspondence to Lewis: jacklewis@suddenlink.net).

Citation: Lewis, J. and R., Coats. 2020. "Trends in Raindrop Kinetic Energy with Modeled Climate Warming in the Lake Tahoe Basin." *Journal of the American Water Resources Association* 1–14. https://doi.org/10.1111/1752-1688.12834.

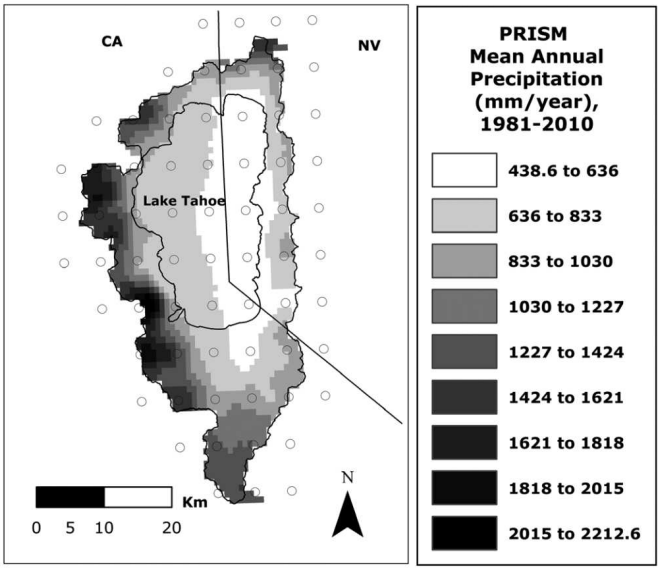

FIGURE 1. Mean annual precipitation in the Tahoe basin, from Parameter-elevation Regressions on Independent Slopes Model (PRISM; Daly et al. 1994). Circles indicate centers of the 1/16 degree grid cells used in the climate models. CA, California; NV, Nevada.

Climatic change is having measureable effects on the lake and its watershed. Since the early 1970s, the lake has been warming at an average rate of about 0.013 °C/yr, and the warming is increasing its thermal stability and resistance to deep mixing (Coats et al. 2006; Sahoo et al. 2013). With increasing air temperature, precipitation is shifting from a snow- to a rain-dominated regime, the spring snowmelt pulse is shifting toward earlier dates, and rainfall intensity and interannual variability are increasing (Coats 2010). Results from down-scaled GCMs have shown that these trends will likely continue, and lead to increases in drought severity, vegetation changes, increased flood risk, and increased nutrient flux to the Lake (Coats et al. 2013; Dettinger 2013; Sahoo et al. 2013). The recent and projected future trends in hydroclimatology of the Tahoe Basin mirror the trends reported for other areas of the western United States (U.S.) (Lettenmaier and Gan 1990; Aguado et al. 1992; Wahl 1992; Pupacko 1993; Cayan et al. 2016).

In the Tahoe Basin, several climate-related factors could drive upward trends in nutrient and sediment loading into Lake Tahoe. The expected shift from snowfall to rainfall in the Tahoe Basin will result in faster runoff and conditions likely to produce (in the short run) rain-on-snow events. The decreasing extent and duration of snowpack will leave unvegetated soils increasingly vulnerable to erosion by rainfall. We expect that risks for rill and gully erosion will increase, and the higher peak streamflows will result in greater stream bank and channel erosion. Higher soil and air temperatures could accelerate mineralization of organic nitrogen and phosphorus, but could also increase tree growth and nutrient uptake, with unpredictable consequences for nutrient loading to the lake.

In this study we focus on the increasing exposure of soils to raindrop impact and the possible increases in frequency and intensity of rainfall (Dominguez et al. 2012; Donat et al. 2016; Prein et al. 2016; Polade et al. 2017), which suggest that rain on snow-free soil will become an increasing source of fine sediment and particulate nutrients to the lake. McCall (2013) projected increases in the kinetic energy of raindrops (KE) based on extrapolation of a 10-year warming trend at one meteorological station near Fallen Leaf Lake in the Tahoe Basin. The purposes of this study were to examine trends in the KE of raindrops under spatially explicit modeled future scenarios of climate change in the Basin, and to evaluate the relative importance of increases in snow-free ground and increases in KE as factors contributing to increases in soil erosion. We used downscaled daily output from four GCMs with historic and two future emissions scenarios together with hourly data from nine recording precipitation gages to calculate trends in annual maximum hourly and total annual KE of raindrops on snow-free ground (MKE and TKE, respectively) at a 6-km grid scale.

The Physics of Raindrops

The two forces acting on the falling drop are the acceleration due to gravity, assumed constant, and the drag force, which is a function of both shape and velocity-squared. As the upward force increases with velocity, the falling drops nearly reach their terminal velocity after falling a short distance.

The KE of a single, large drop of a given volume at terminal velocity is greater than the sum of energies of a number of smaller drops of equal total volume, since less energy is dissipated in overcoming air resistance by the larger drop. A 6.0 mm drop has 2.16 times the KE of the same mass of 1.5 mm droplets (*ceteris paribus*), and this energy is concentrated at a single point of impact (McCall 2013). Factors not considered include updrafts, downdrafts, and air density.

Density of raindrops in air can vary from 1,000 to more than 5,000 raindrops per cubic meter depending on the intensity of a particular rainfall event (Blanchard 1967, cited by Dohrenwend 1977). Intensity of rainfall is thus a function of variations in drop-size distributions during an event and the number of drops.

There is a direct relationship between rainfall intensity and KE. Using direct measurements of drop-size distributions, Sempere-Torres (1992) explored the relationship between KE and rainfall intensity, testing nine common formulae in two storms of about 3,000 min with intensities up to 90 mm/hr. They found that the relationship varies over the rainfall intensity range. At low intensities, large drops are rare, but as drop size increases with increasing intensity, the slope of the relationship increases. Above a threshold of about 20 mm/hr, the drop-size distribution is no longer relevant and the KE is explained very well ($R = 0.97$) by a linear regression on rainfall intensity. For a 1-min duration, Sempere-Torres (1992) found that the KE (J/m^2) for a rainfall of intensity I (mm/hr) is approximated by the following equation:

$$\mathrm{KE} = 0.56I - 3.1. \quad (1)$$

The KE of falling rain has a direct influence on the detachment and initial transport of soil particles. Sealing of the soil surface increases with increasing energy of falling rain (Dohrenwend 1977), contributing to rill erosion. KE tends to overestimate the erosion potential of low-intensity rainfall, as smaller drops are less effective at detaching soil, whereas at high intensities, saturation and shallow ponding may increase the efficiency of detachment (Van Dijk et al. 2002). Figure 2 shows soil particles dislodged by raindrops during an intense event and splashed onto a vertical board installed on bare soil at a soil erosion study plot in the Tahoe Basin.

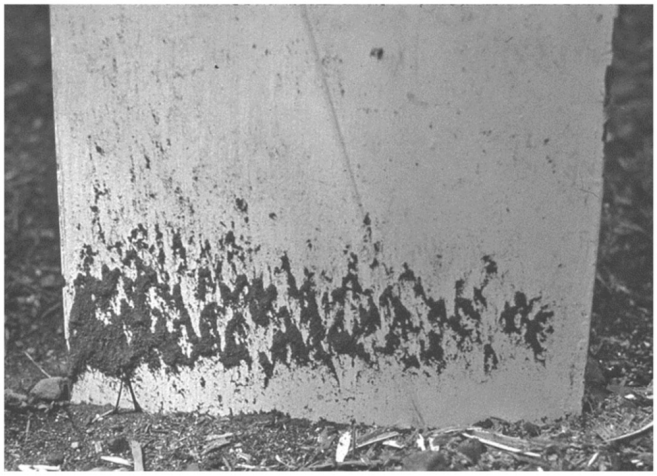

FIGURE 2. Soil particles dislodged by raindrops during an intense event and splashed onto a vertical board installed on bare soil at a soil erosion study plot in the Tahoe basin. Photo by R. Coats, 1974.

METHODS

Study Area

Mean annual precipitation in the Tahoe Basin ranges from >200 cm/yr on the west side of the basin to <50 cm/yr near the Lake on the east side (Figure 1). Most of the precipitation at higher elevations falls as snow between November and April, but elevations near the lake are in a rain-snow transition zone. Rainfall combined with snowmelt during "atmospheric river" events (Konrad and Dettinger 2017) account for the largest floods. Most of the annual runoff historically occurs in late spring and early summer. In some years, summertime monsoonal storms bring intense rainfall, especially at high elevations on the east side of the basin.

Soils of the basin are derived from andesitic volcanic rocks and granodiorite, with minor areas of metamorphic parent materials. Valley bottoms are mantled with glacial moraines or glacial outwash debris derived from the parent rock. The basin soils (in the <2 mm fraction) are 65%–85% sand (Rogers 1974). Vegetation is dominated by a mixed conifer forest of Jeffrey pine (*Pinus jeffreyi*), lodgepole pine (*P. murrayana*), white fir (*Abies concolor*), and red fir (*A. magnifica*). There are significant areas of wet meadow, dry meadow, brush fields, and rock outcrop.

About six percent of the basin land area has been developed for residential and commercial uses, especially along the north, south, and west shores. The rate of development was especially intense during the 1960s and 1970s, but has since slowed due to land use controls.

Data Sources

Four GCMs (HadGEM2-ES, CNRM-CM5, CanESM2, and MIROC5) and two greenhouse gas (GHG) trajectories (RCP4.5 and RCP8.5) were selected by the Southwest Climate Science Center (SWCSC) to cover a range of temperature and moisture trends for the Tahoe Basin (Pierce et al. 2018). Using the method of Localized Constructed Analogues (LOCA) (Pierce et al. 2014), the daily precipitation and temperature (T_{max} and T_{min}) data were downscaled for us by SWCSC to a 1/16th degree (*ca.* 6 km) grid for the Basin, and adjusted using a frequency-dependent bias correction (Pierce et al. 2015). The downscaled LOCA data were "trained" to the Livneh et al. (2015) gridded temperature and precipitation data. SWCSC then used the corrected LOCA data as input to the Variable Infiltration Capacity (VIC) model (Liang and Lettenmaier 1994; Hamman et al.

2018; Pierce et al. 2018), producing as output a suite of 23 hydrologic and meteorological variables, including daily precipitation, daily rainfall, and snow water equivalent (SWE) of any snowpack. A historic time period (1950–2005) was included for each model, and the future (2006–2099) was projected for each model/scenario combination. It must be noted that the RCP4.5 scenario seems increasingly unrealistic, since the estimated GHG emissions are now exceeding the rate projected by RCP8.5 (IPCC 2018).

Disaggregating Daily Rainfall on Snow-Free Ground to Hourly Rainfall KE

The average daily KE of raindrops can be estimated from daily rainfall, but of much more interest are the KE values calculated from short-duration rainfall intensities. Hourly data for temperature and precipitation are available from a network of nine snow telemetry (SNOTEL) gages in or near the Tahoe Basin (Natural Resource Conservation Service 2017) for the period 2008–2016 (Figure 3).

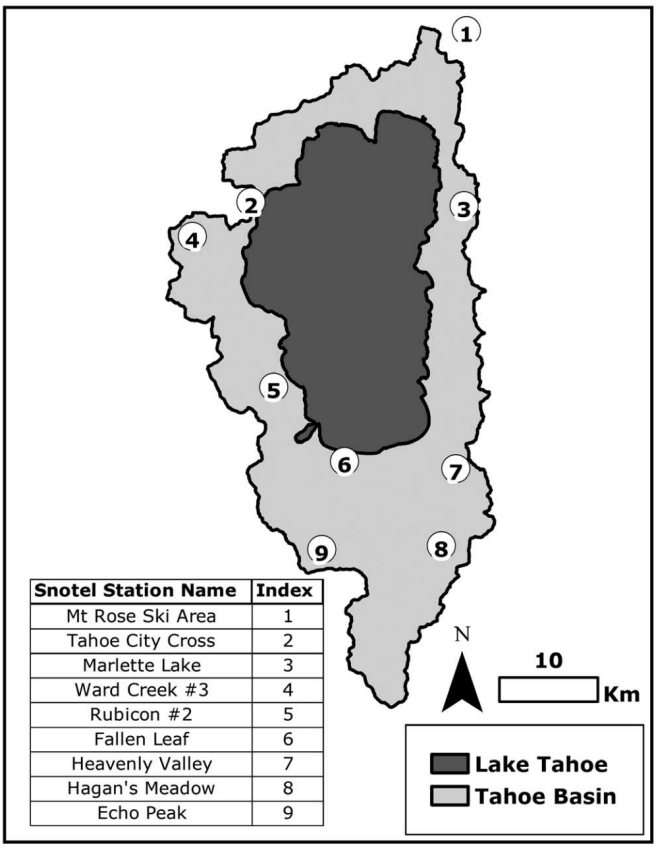

Snotel Station Name	Index
Mt Rose Ski Area	1
Tahoe City Cross	2
Marlette Lake	3
Ward Creek #3	4
Rubicon #2	5
Fallen Leaf	6
Heavenly Valley	7
Hagan's Meadow	8
Echo Peak	9

FIGURE 3. Locations of snow telemetry hourly-recording precipitation stations in the Tahoe Basin.

To eliminate snowfall from KE calculations, we first filtered out precipitation that fell when the hourly temperature was at or below 0°C. For each of the 44 cells over land in the basin, we then disaggregated the modeled daily rainfall on snow-free ground (i.e., on days when the SWE in the cell was <1 mm) to hourly values using observations from the nearest SNOTEL station (identified using the Near tool in ArcGIS10, ESRI 2018). Modeled days were matched to SNOTEL days selected at random from days with similar rainfall totals (as described below), and the SNOTEL hourly rainfall was multiplied by a constant to exactly match the modeled daily rainfall.

Days with modeled rainfall less than the 2.54-mm (0.1 in.) resolution of SNOTEL data were excluded. We used an iterative matching procedure that sought to select from at least four days with similar totals in the SNOTEL record for the modeled month. When the modeled future rainfall exceeded the maximum historic SNOTEL daily rainfall for that month by at least 100%, the day of that maximum was selected rather than making a random selection.

For each year, the TKE and MKE from the disaggregation was saved. To approximate hourly KE at intensities >20 mm/hr we multiplied Equation (1) above by 60 min/hr, yielding $KE = 33.6I - 186$ in J/m^2/hr. Since the relationship is linear, no error is introduced by assuming constant intensity until intensity falls below 20 mm/hr. For rainfall intensities up to 20 mm/hr, the Wischmeier and Smith (1958) relationship, expressed in metric units (equation 2 in Sempere-Torres 1992), was rescaled to be continuous with the high-intensity relation at $I = 20$ using a multiplier of 1.0448:

$$KE = 1.0448I(11.9 + 8.73 \log I). \quad (2)$$

Since relationship (Equation 2) is nearly linear (Figure 4) the constant intensity assumption used in employing Equation (1) introduces very little error even at low intensities.

Because of the coarse resolution in the SNOTEL data, temporal disaggregation is not very realistic for days with less than about 5 mm of rainfall, because in such cases all the rainfall is assigned to one or two hours. The elimination of modeled rainfall <2.54 mm per day results in a systematic underestimation of TKE but should have no effect on our trend analyses for either TKE or MKE.

The disaggregation is also spatially unrealistic because it is done independently for each 6-km grid cell. The lack of realistic spatial autocorrelation should have no systematic effect on TKE or MKE for any given cell, and therefore should have no systematic effect on means of cells, averaged over the Tahoe Basin or subbasins.

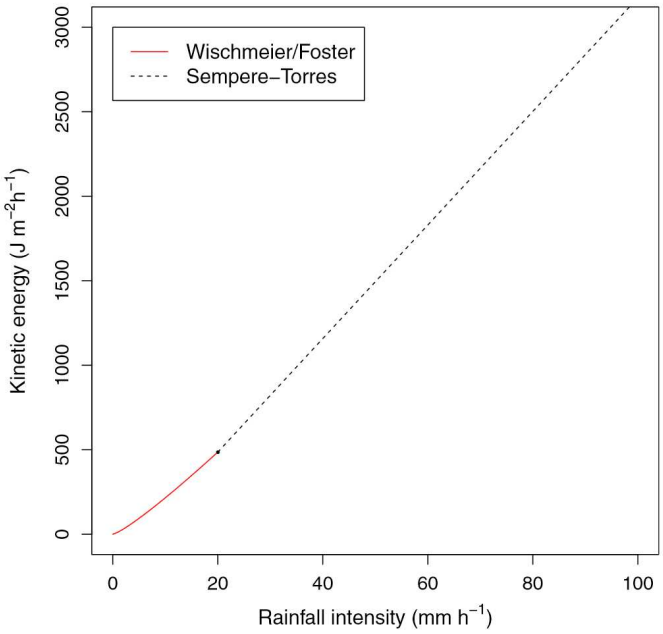

FIGURE 4. Relation between kinetic energy (KE) and rainfall intensity defined by Equation (1), multiplied by 60 to yield hourly rainfall, KE = $33.6I - 186$ for $I > 20$, and Equation (2) KE = $1.0448I\,(11.9 + 8.73 \log I)$ for $0 < I \leq 20$.

Rain-on-Snow

Though our focus in this study is rain on bare soil, some readers may be interested in its complement: rain-on snow (ROS). Such events are implicated in the occurrence of large floods in the Sierra Nevada (Kattelmann 1997). Only one of the models we have considered suggests an increase in total rain on snow and three of the models predict a decrease in the number of rain on snow events (days). A brief discussion of the significance and time trends in ROS events is included in Supporting Information.

Model Scenarios

Scenarios included modeled historic (HIST) atmospheric conditions (using measured GHG concentrations, 1950–2005), and future GHG concentrations under RCP4.5 and RCP8.5 (2006–2100). We focus here on two scenarios encompassing pooled historic and future conditions (H + RCP4.5 and H + RCP8.5). Time series for the individual cells were averaged across the Tahoe Basin and over western and eastern subregions of the basin. For each GCM and scenario, statistical distributions were fitted to the time series for the whole basin and the two subregions. To describe average behavior across models, return level curves derived from the fitted statistical distributions were averaged over the four GCMs.

Analyzing Trends with the Generalized Extreme Value Distribution

Time trends of MKE and TKE were analyzed using the Generalized Extreme Value distribution (GEV df). The GEV df (Coles 2001) is theoretically justified for fitting to maxima of long blocks of data such as annual maxima of hourly raindrop energy (MKE), but not TKE. Nevertheless, GEV sometimes fit TKE reasonably well; when it did not we found that in most cases it fit well to the logarithm of TKE. The GEV df has three parameters: (1) the location μ governs central tendency, (2) the scale σ governs dispersion, and (3) the shape ξ governs tail behavior of the distribution. There are three special cases of the GEV df, depending on the sign of the shape parameter (Gilleland and Katz 2016): (1) the heavy-tailed Fréchet df ($\xi > 0$), (2) the upper-bounded reverse Weibull df ($\xi < 0$), and (3) the Gumbel df (limiting case as $\xi \to 0$).

The extRemes package (Gilleland 2016; Gilleland and Katz 2016) in R (R Core Team 2017) implements methods for stationary and nonstationary extreme value analysis including GEV-fitting. For nonstationary distributions, extRemes makes it possible to model the parameters of the GEV as linear or polynomial functions of time (or other covariates). As we were fitting multiple time series, we used an automated procedure to choose among the following five models:

1. Stationary
2. Linear location parameter
3. Quadratic location parameter
4. Linear location and linear scale parameters
5. Quadratic location and linear scale parameters

Gilleland and Katz (2016) note that varying the scale parameter without varying the location parameter is generally not recommended, so we did not consider a linear scale parameter by itself. We wanted a more stringent criterion than Akaike's information criterion (AIC; Sakamoto et al. 1986) for adding complexity to the model, so additional parameters were accepted only when likelihood ratio (LR) tests favored their inclusion at the 5% significance level. LR tests were used to compare models 1–2, 2–3, 2–4, and 3–5. AIC was used to select between models 3 and 4 (which have the same number of parameters).

Goodness-of-fit of empirical and modeled distributions was compared using quantile–quantile plots and density plots (e.g., Figure 5). Time trends were visualized by overlaying curves for the 2-, 20-, and 100-year return levels on time series scatterplots of the response variables: MKE and TKE. We applied the nonparametric Mann–Kendall tau test (Mann 1945;

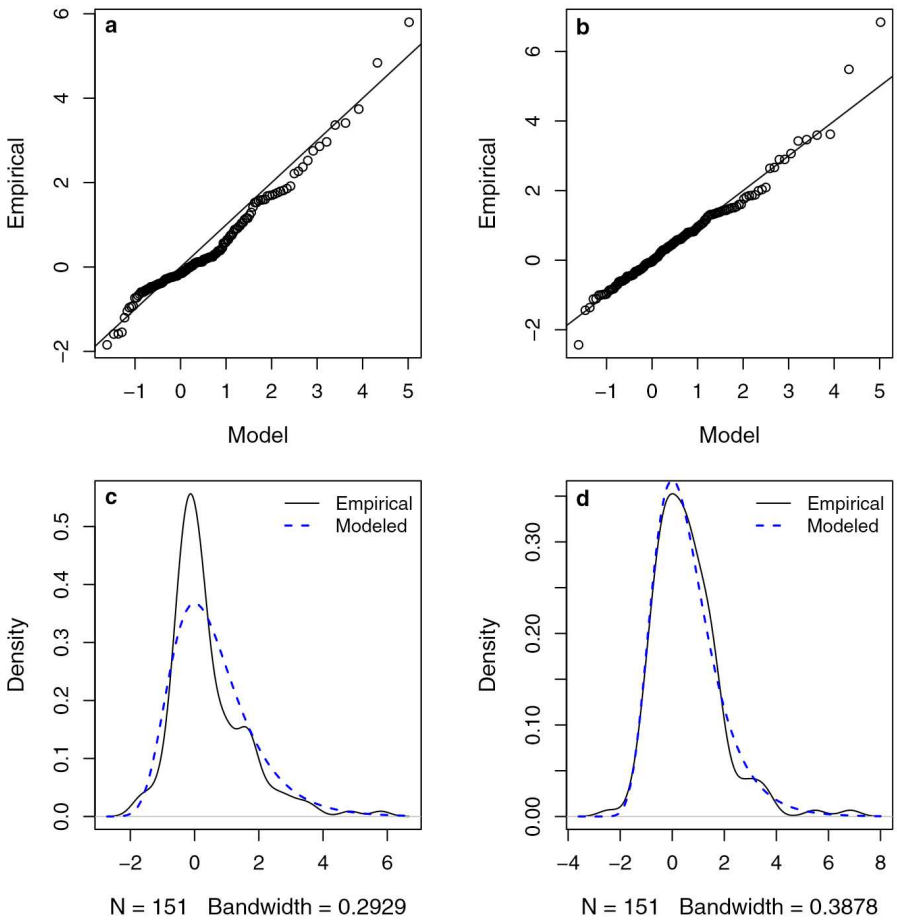

FIGURE 5. Quantile–quantile plots (a,b) and density plots (c,d) of the GEV df fitted to TKE (a,c) and the logarithm of TKE (b,d) for model CanESM2 under scenario H + RCP8.5. GEV, Generalized Extreme Value; TKE, total kinetic energy.

Helsel and Hirsch 2002) to evaluate the significance of trends and a nonparametric *loess* curve (LOcal RegrESSion) (Cleveland 1979) was added to each scatterplot. The loess curve approximates the mean for any given year, so for symmetrical distributions it corresponds well with the two-year return level curve, which is the median of the statistical distribution. It may therefore be interpreted as another indication of goodness-of-fit for the model used to estimate return levels.

Separating Effects of Increased Rain Intensity from Effects of Reduced Snow Cover

Since we are interested in the trends in raindrop KE on snow-free terrain, we filtered out precipitation for days and locations with a significant snowpack. Our trends thus provide a view of effects of climate change on surface erosion hazard, but beg the question: are the observed trends due to increased raindrop energy, or to loss of snow cover? To separate the effects of raindrop energy and snow cover, we repeated the analysis for detrended mean snow cover. For each modeled year (historic and future), a random year from the period 1950 to 2005 was selected (with replacement), and the SWE for each cell and date of that year was substituted for the actual SWE. [Note: for leap years, only leap years were re-sampled.] We then repeated the prior analysis: (1) replacing modeled rainfall with zero, for days and grid cells in which SWE was at least 1 mm; (2) disaggregating to hourly rainfall using the SNOTEL gage data; (3) recomputing MKE and TKE each year; (4) averaging results across cells; and, (5) analyzing the trends using the GEV df.

Magnitude of change was compared for the original analysis and the analyses based on detrended snow cover. This process was carried out for the HadGEM2 and CanESM2 models combining historic years and a future based on RCP8.5. These combinations of model and scenario were selected for their contrasting shape and magnitude of trend in MKE and TKE (Figures 6 and 7).

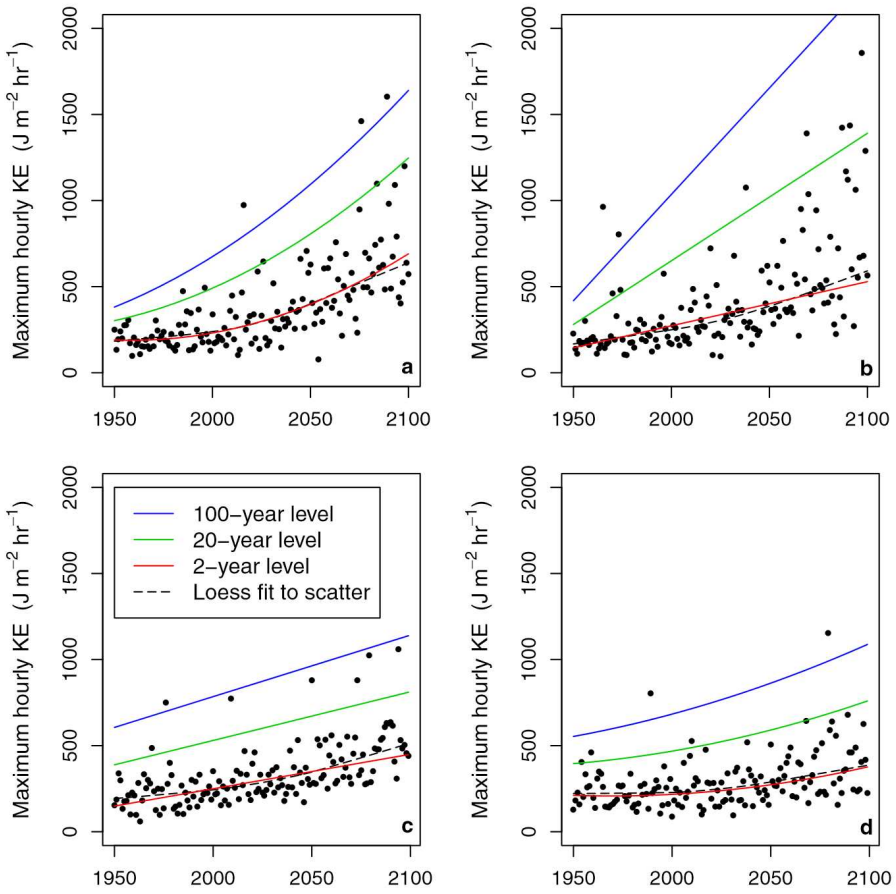

FIGURE 6. Modeled maximum hourly KE (MKE) under scenario H + RCP8.5 for four climate models: (a) CanESM2, (b) CNRM, (c) HadGEM2, and (d) MIROC5. Return levels are based on GEV df fitted to untransformed MKE.

RESULTS AND DISCUSSION

Trends in MKE and TKE

For both response variables, models CanESM2 and CNRM predicted greater increases in magnitude and variability than HadGEM2, whereas MIROC5 predicted the least and slowest change (Figures 6 and 7). For all models, we found little or no trend in the historic data for both responses and, in most cases, slightly greater trends for RCP4.5 than for historic climate. The pooled scenario H + RCP4.5 generally exhibited modest increases and, predictably, trends were stronger for H + RCP8.5 (Figure 8). Under H + RCP8.5, the return levels for TKE triple between the years 2000 and 2075, increasing five-fold by 2100. The corresponding factors for MKE from 2000 to 2100 are 2.6, 2.2, and 2.1, respectively, for return levels of 2, 20, and 100 years. The GEV df generally provided good fits to MKE and to the logarithm of TKE. Some of the two-year curves for TKE rise faster than the loess smoother toward the end of the modeled period (Figure 7a, 7c, 7d), suggesting that, despite diagnostic plots indicating good fits to the GEV df, the rate of increase in the late 21st Century may be overestimated.

Spatial Distribution of Trends in KE

Percent changes in MKE seem to be greatest near the lake for H + RCP4.5 and lowest in the southern portion of the basin for H + RCP8.5 (Figure 9). The greatest spatial contrast in magnitudes of KE resulted from topographically controlled precipitation differences between the west side of the basin and the drier east side. Projections of MKE are similar on both sides of the basin under scenario H + RCP8.5 (Figures 9 and 10), with all return levels of MKE for a given return interval approximately doubling between 2005 and 2100. TKE rises even more dramatically, with return TKE levels increasing four- to five-fold. The increases in TKE were slightly larger on the west side than on the east. The mean ratio of TKE on the west side relative to the east side

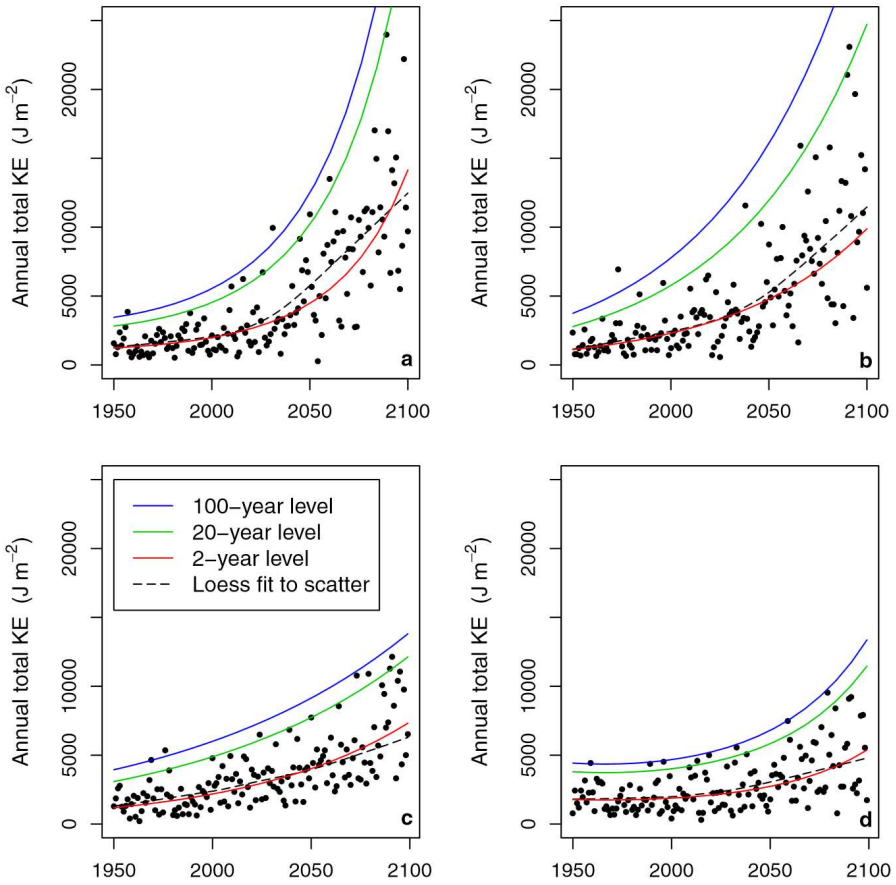

FIGURE 7. Modeled TKE under scenario H + RCP8.5 for four climate models: (a) CanESM2, (b) CNRM, (c) HadGEM2, and (d) MIROC5. Return levels are based on GEV df fitted to the logarithm of TKE.

increased from 1.65 in the first 50 years to 1.94 in the final 50 years.

Separating the Effects of Trends in Raindrop Energy from Trends in Snowpack

The dashed lines and hollow circles show the results for snow cover detrended by resampling, overlaid on the original results (Figure 11). Resampling the SWE gave rise to a small increase in both MKE and TKE, which is apparent for the years 1950–2000. This is likely due to the decoupling of precipitation and snowpack, as high rainfall years are more likely to be paired with low snowpack years, leading to more years of high KE than might be realistic. However, the effect of a shrinking snowpack becomes more important starting around 2010–2020 and the curves for the detrended snowpack drop below the steeper curves for the shrinking snowpack. Nevertheless, the curves for MKE do rise in the 21st Century under CanESM2 and H + RCP8.5, even for the detrended snowpack, indicating that changes in both raindrop energy and snowpack are important factors behind the increases in raindrop KE on bare soil. In contrast, under the HadGEM2 pooled H + RCP8.5 scenario, without including the snowpack trend there is no trend in MKE and only a barely detectable trend in TKE. This result is consistent with the near absence of changes in rainfall intensity under HadGEM2, which predicts no trends in annual or 30-day maximum precipitation, and only a very subtle trend in maximum daily precipitation (1 mm per decade under HadGEM2 versus 2.3 mm per decade under CanESM2).

Under CanESM2, the changes from 1950 to 2100 in the two-year return level for MKE are 263% for the original analysis compared to 104% for that with detrended snow cover. The 20-year return levels more than quadrupled for the original analysis, and approximately doubled with detrended snow cover. The 20- and 100-year return levels for TKE increased by 1,000% in the original analysis compared to only 35% and 25%, respectively, with detrended snow cover.

Under HadGEM2, the changes from 1950 to 2100 in the two-year return level for MKE are 200% for

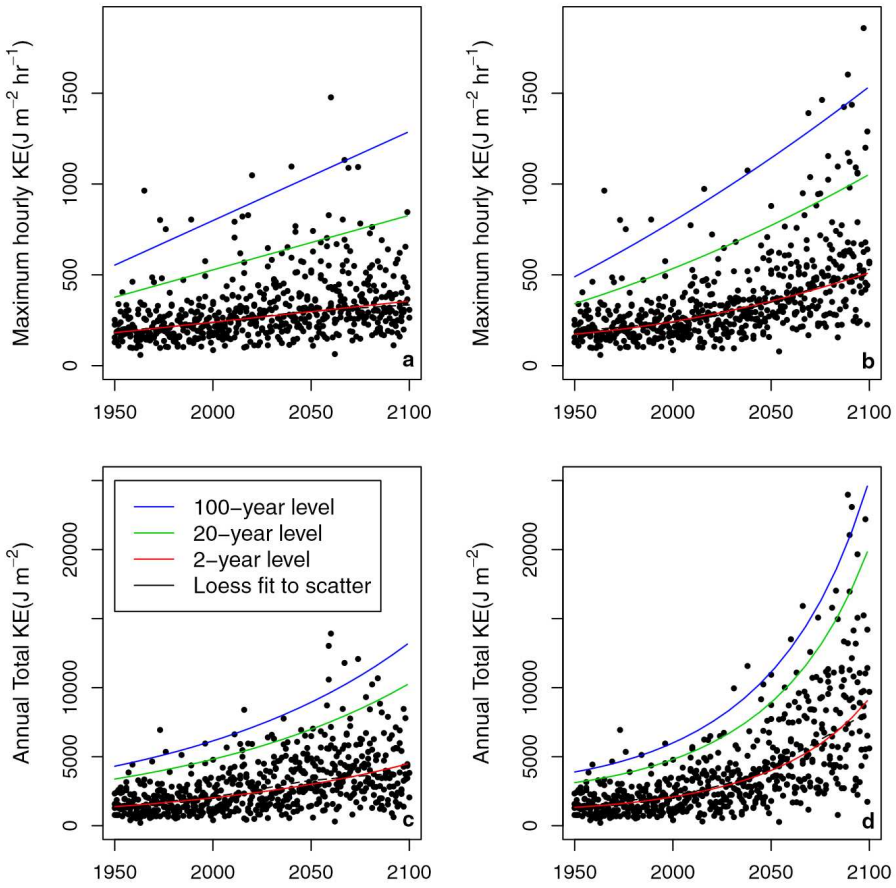

FIGURE 8. Modeled annual maximum hourly (a,b) and total annual (c,d) raindrop energy on snow-free ground, scenario H + RCP4.5 (a,c) and H + RCP8.5 (b,d), showing predictions from all four general circulation models (GCMs). Return levels for each GCM were calculated with the GEV df fitted to the MKE and the logarithm of TKE. For each recurrence interval, plotting points were averaged over GCMs to produce these curves, for example, the curves in frame (b) are the averages of the curves in the four frames of Figure 6.

the original analysis compared to 18% with the detrended snow cover, whereas changes in TKE are 519% for the original analysis compared to 53% for the detrended snow cover. The 20-and 100-year trend lines for MKE roughly doubled for the original analysis, whereas changing <10% with detrended snow cover. The 20-and 100-year trend lines for TKE rose 294% and 250%, respectively, for the original analysis, whereas rising 53% with detrended snow cover.

Implications for Soil Erosion and for Other Locations

The Water Erosion Prediction Project model relates interrill surface erosion to rainfall intensity, soil erodibility, and hillslope gradient. Not only are rainfall intensity and KE very closely related (Sempere-Torres 1992), but empirical results suggest a power law relating soil erodibility to raindrop KE (Moussouni et al. 2014). Hence soil erosion is strongly influenced by rainfall KE.

These results have implications for mountainous regions throughout the western U.S. and many other regions where warm temperatures are expected to result in more precipitation as rainfall and reduced duration and extent of snowpack.

Sources of Uncertainty

As with most analyses, there are uncertainties associated with each step. These include:

1. Variability between runs of a given GCM (internal variability). We used just one run of each GCM.
2. Selection of GCMs. We used models that were selected by the SWCSC to cover a range of trends. Variability among models is greater than internal variability (Deser et al. 2016; David Pierce, Scripps Institution of Oceanography, July 2019, personal communication). All models agree that increases in both MKE and

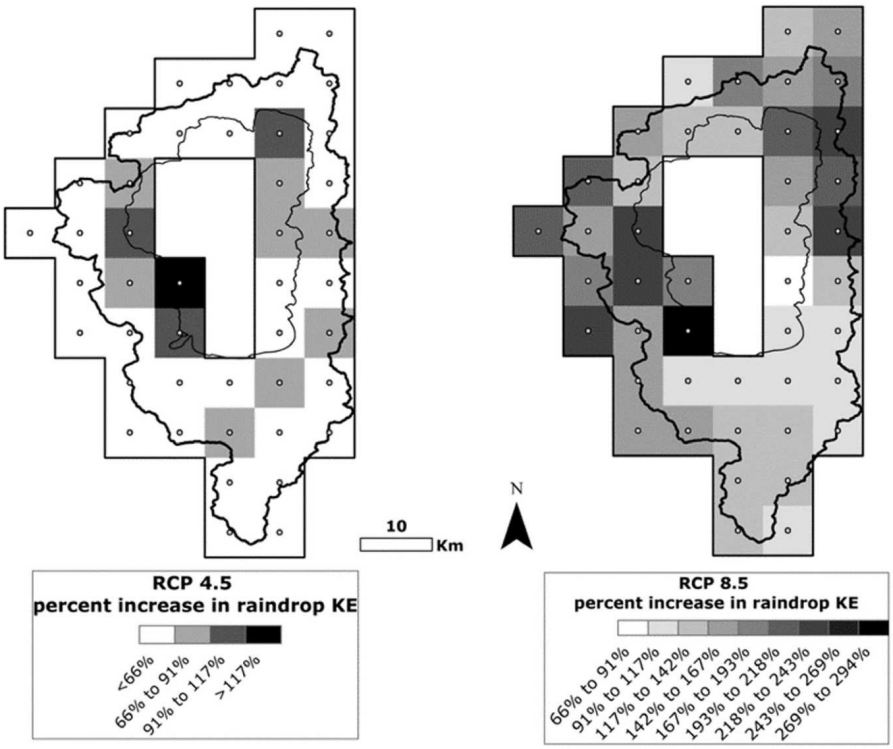

FIGURE 9. Percent change in average of annual maximum hourly raindrop energy on snow-free ground ($J/m^2/hr$) from modeled historic period to modeled years 2070–2099, at grid cells covering the land in the Tahoe basin. Note that the shading for RCP4.5 and 8.5 are different.

TKE will occur. Uncertainty due to model selection would mainly affect rate and magnitude of change, and the importance of changing rainfall inputs.

3. Downscaling from the GCM lat-long grid (100–300 km) to approximately 6 km for input to VIC.
4. VIC generation of hydrometeorological variables.
5. Disaggregation from daily to hourly time step. Hourly rainfall amounts at nine SNOTEL gages were rescaled to match modeled daily totals, hence this only affected the intradaily temporal distribution of rainfall. TKE is insensitive to the hourly distribution, so uncertainty introduced at this step would primarily affect MKE.
6. Conversion of I to KE. These two quantities are closely related ($r = 0.97$ above 20 mm/hr). Based on the regression scatter (figure 3 in Sempere-Torres 1992), this source of error is very small (<0.5 J/m^2)
7. Selection, fitting, and parameterization of the GEV df. Goodness-of-fit to this distribution varied among runs and scenarios and was affected by the choice of variable transformation as well as the parameterization of the location and scale factors of the GEV df. This uncertainty affects return level estimates and trends (e.g., Figure 7a).
8. Trajectory of GHG emissions. While RCP8.5 appears to be a much more likely trajectory than RCP4.5, no one knows how close it will be to reality.

While there are many sources of uncertainty in the results, none are great enough to affect the following conclusions.

SUMMARY AND CONCLUSIONS

The potential for increased erosion and transport of nutrients and sediment into Lake Tahoe is growing as the climate warms. Variability of transport will increase as its magnitude increases. The mechanisms of change we have investigated are a shift in precipitation from snow to rain and a reduction in the duration of snow cover, which protects the soil from erosion by raindrop impact. Effects are relatively subdued under the RCP4.5 GHG concentration scenario, but are dramatic under RCP8.5. All four models concurred that these changes will occur. Based on the average behavior of the four models, 2- to 200-year return levels for MKE will at least double during the

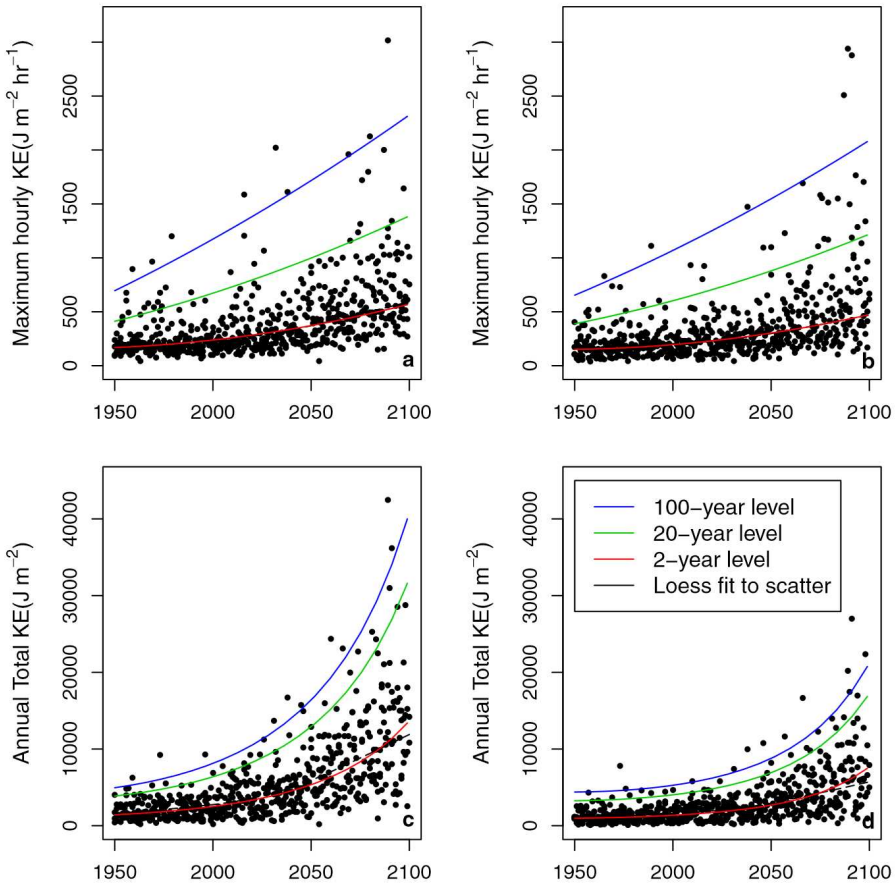

FIGURE 10. Modeled annual maximum hourly (a,b) and total annual (c,d) raindrop energy on snow-free ground for scenario H + RCP8.5, west side (a,c) and east side (b,d) of the Tahoe basin, showing predictions from all four GCMs. Return levels for each GCM were calculated with the GEV df fitted to MKE and the logarithm of TKE. For each recurrence interval, plotting points were averaged over GCMs to produce these curves.

21st Century, whereas those for TKE will more than triple. Indications are that reduction in snow cover is the primary driving factor. Changing rainfall inputs are also important according to CanESM2, but may be unimportant according to the HadGEM2 model. The west side of the basin receives more precipitation than the east side of the basin, so the KE due to raindrops on snow-free ground is greatest there, but relative changes are similar on the west and east sides of the basin.

The sensitivity of Lake Tahoe's clarity to inputs of nitrogen, phosphorus, and fine sediment is well established (Goldman 1988; Jassby et al. 2003). Since the early 1970s, control of degradation of the Lake's water quality has been the focus of major research, monitoring, and regulatory programs (Schuster and Grismer 2004; Roberts and Reuter 2007). These programs must now deal not only with the legacy and future impacts of land development in the Tahoe Basin, but also with the impacts of accelerated surface erosion on bare soil resulting from climate change. Although the causes of climate change must be addressed at the national and international scale, Best Management Practices (BMPs) for controlling the load of nutrients and fine sediment to the Lake have been developed, applied, and tested in the Tahoe Basin. These BMPs include mulching of disturbed soil on road-cuts (Grismer and Hogan 2004, 2005), and use of detention basins to trap runoff from developed areas (Heyvaert et al. 2007) Ultimately the effectiveness of these efforts will depend not just on science and technology, however, but also on the dedication and will of public agency staffs, political leaders, and residents of the Basin.

SUPPORTING INFORMATION

Additional supporting information may be found online under the Supporting Information tab for this article: (1) complete set of model projections, (2) projected changes in precipitation falling as rain on

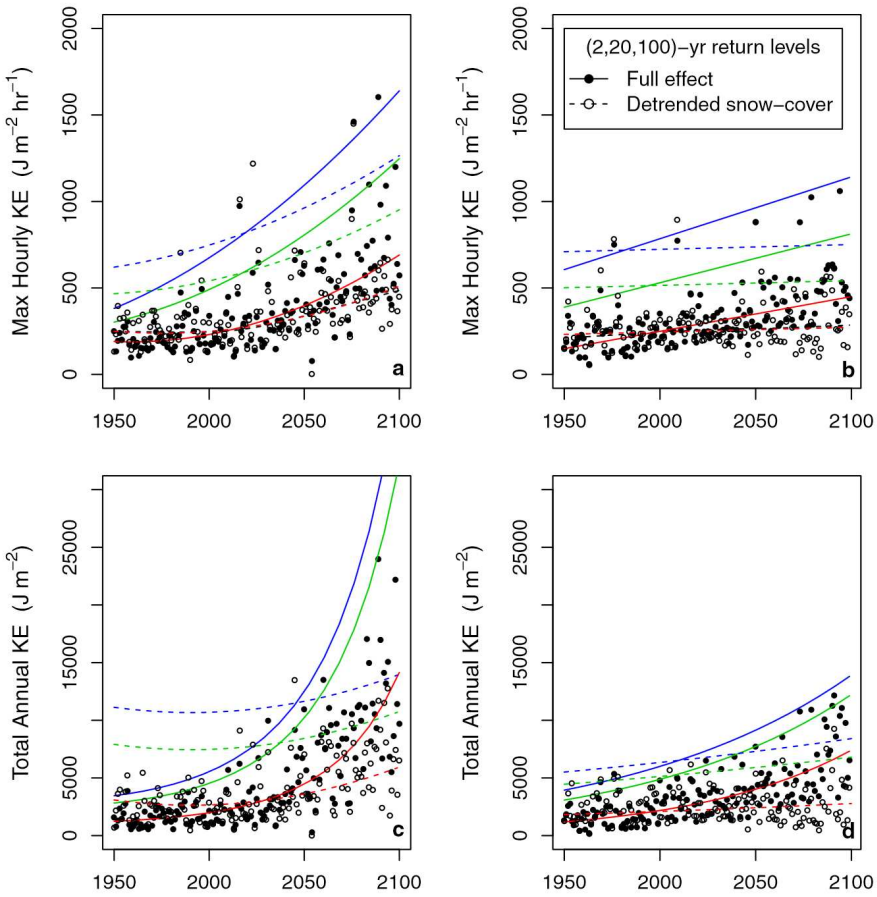

FIGURE 11. Modeled annual maximum hourly (a,b) and total annual (c,d) raindrop energy on snow-free ground, scenario H + RCP8.5, with and without a trend in snow cover, for CanESM2 (a,c) and HadGEM2 (b,d). Return levels for hourly KE were calculated with the GEV df fitted to MKE and the logarithm of TKE, with one exception: in frame (c) the GEV df was fitted to the untransformed TKE for calculating trends without a snow cover (dashed curves).

snow, and (3) comparison of modeled historic with measured precipitation at Tahoe City.

ACKNOWLEDGMENTS

We thank David Pierce and Daniel Cayan of the Scripps Institution of Oceanography SWCSC for providing the downscaled GCM and VIC output; Goloka Sahoo of the Tahoe Environmental Research Center for data formatting; Zachary Silber-Coats for making the maps with ArcGIS 10; and Katherine McCall for suggesting that we examine raindrop KE. This work was funded in part by a grant from the California Tahoe Conservancy.

LITERATURE CITED

Aguado, E., D. Cayan, L. Riddle, and M. Roos. 1992. "Climatic Fluctuations and the Timing of West Coast Streamflow." *Journal of Climate* 5: 1468–83.

Blanchard, D. 1967. *From Raindrops to Volcanos*. New York, NY: Doubleday.

Cayan, D., M. Dettinger, D. Pierce, T. Das, N. Knowles, F. Ralph, and E. Sumargo. 2016. "Natural Variability, Anthropogenic Climate Change, and Impacts on Water Availability and Flood Extremes in the Western United States." In *Water Policy and Planning in a Variable and Changing Climate*, edited by K. Miller, A. Hamlet, D. Kelly, F. Ralph, and K. Redmond, 17–44. Boca Raton, FL: Taylor & Francis Group, CRC Press.

Cleveland, W.S. 1979. "Robust Locally Weighted Regression and Smoothing Scatterplots." *Journal of the American Statistical Association* 74: 829–36.

Coats, R. 2010. "Climate Change in the Tahoe Basin: Regional Trends, Impacts and Drivers." *Climatic Change* 102: 435–66. https://doi.org/10.1007/s10584-010-9828-3.

Coats, R., M. Costa-Cabral, J. Riverson, J. Reuter, G. Sahoo, G. Schladow, and B. Wolf. 2013. "Projected 21st Century Trends in Hydroclimatology of the Tahoe Basin." *Climatic Change* 116: 51–69.

Coats, R., J. Perez-Losada, G. Schladow, R. Richards, and C.R. Goldman. 2006. "The Warming of Lake Tahoe." *Climatic Change* 76: 121–48.

Coles, S. 2001. *An Introduction to Statistical Modeling of Extreme Values*. Berlin: Springer-Verlag.

Daly, C., R. Neilson, and D. Phillips. 1994. "A Statistical-Topographic Model for Mapping Climatological Precipitation over Mountainous Terrain." *Journal of Applied Meteorology* 33: 140–58.

Deser, C., L. Terray, and A. Phillips. 2016. "Forced and Internal Components of Winter Air Temperature Trends over North America during the Past 50 Years: Mechanisms and

Implications *Journal of Climate* 29 (6): 2237–58. https://doi.org/10.1175/JCLI-D-15-0304.1.

Dettinger, M.D. 2013. "Projections and Downscaling of 21st Century Temperatures, Precipitation, Radiative Fluxes and Winds for the Southwestern US., with Focus on the Lake Tahoe Basin." *Climatic Change* 116: 17–33.

Dohrenwend, R. 1977. *Raindrop Erosion in the Forest*. L'Anse, MI: Michigan Techological University Ford Forestry Center.

Dominguez, F., E. Rivera, D. Lettenmaier, and C. Castro. 2012. "Changes in Winter Precipitation Extremes for the Western United States under a Warmer Climate as Simulated by Regional Climate Models." *Geophysical Research Letters* 39: L05803.

Donat, M., A. Lowry, L. Alexander, P. O'Gorman, and N. Maher. 2016. "More Extreme Precipitation in the World's Dry and Wet Regions." *Nature Climate Change* 6: 508–13. https://doi.org/10.1038/NCLIMATE2941.

ESRI. 2018. *ArcGIS Desktop: Release 10.6*. Redlands, CA: Environmental Systems Research Institute.

Gilleland, E. 2016. "extRemes: Extreme Value Analysis. R Package Version 2.0-8." https://CRAN.R-project.org/package=extRemes.

Gilleland, E., and R. Katz. 2016. "extRemes 2.0: An Extreme Value Analysis Package in R." *Journal of Statistical Software* 72: 39.

Goldman, C. 1988. "Primary Productivity, Nutrients, and Transparency during the Early Onset of Eutrophication in Ultra-Oligotrophic Lake Tahoe, California-Nevada." *Limnology and Oceanography* 33: 1321–33.

Grismer, M., and M. Hogan. 2004. "Simulated Rainfall Evaluation of Revegetation/Mulch Erosion Control in the Lake Tahoe Basin–1: Method Assessment." *Land Degradation and Development* 15: 573–88.

Grismer, M., and M. Hogan. 2005. "Simulated Rainfall Evaluation of Revegetation/Mulch Erosion Control in the Lake Tahoe Basin–3: Soil Treatment Effects." *Land Degradation and Development* 16: 489–501.

Hamman, J., B. Nijssen, T.J. Bohn, D.R. Gergel, and Y. Mao. 2018. "The Variable Infiltration Capacity Model Version 5 (VIC-5): Infrastructure Improvements for New Applications and Reproducibility." *Geoscientific Model Development* 11: 3481–96. https://doi.org/10.5194/gmd-11-3481-2018.

Helsel, D., and R. Hirsch. 2002. *Statistical Methods in Water Resources Techniques of Water Resources Investigations*. Washington, D.C.: U.S. Geological Survey.

Heyvaert, A., J. Reuter, and C. Goldman. 2007. "Subalpine, Cold Climate, Stormwater Treatment with a Constructed Surface Flow Wetland." *Journal of the American Water Resources Association* 42: 45–54.

IPCC. 2018. Press Release. https://www.ipcc.ch/2018/10/08/summary-for-policymakers-of-ipcc-special-report-on-global-warming-of-1-5c-approved-by-governments/.

Jassby, A., J.E. Reuter, and C.R. Goldman. 2003. "Determining Long-Term Water Quality Change in the Presence of Climatic Variability: Lake Tahoe (USA)." *Canadian Journal of Fisheries and Aquatic Sciences* 60: 1452–61.

Kattelmann, R.1997. "Flooding from Rain-On-Snow Events in the Sierra Nevada. In Destructive Water: Water-Caused Natural Disasters, their Abatement and Control." *Proceedings of the Conference*, Anaheim, CA, June 1996. IAHS Publ no. 239.

Konrad, C., and M. Dettinger. 2017. "Flood Runoff in Relation to Water Vapor Transport by Atmospheric Rivers of the Western United States, 1949–2015." *Geophysical Research Letters*. https://doi.org/10.1002/2017GL075399.

Lettenmaier, D.P., and T.Y. Gan. 1990. "Hydrologic Sensitivities of the Sacramento-San Joaquin River Basin, California, to Global Warming." *Water Resources Research* 26: 69–86.

Liang, X., and D. Lettenmaier. 1994. "A Simple Hydrologically Based Model of Land Surface Water and Energy Fluxes for General Circulation Models." *Journal of Geophysical Research* 99: 14415.

Livneh, B., T.J. Bohn, D.W. Pierce, F. Muñoz-Arriola, B. Nijssen, R. Vose, D.R. Cayan, and L. Brekke. 2015. "A Spatially Comprehensive, Hydrometeorological Data Set for Mexico, the U.S., and Southern Canada 1950–2013." *Scientific Data* 2 (1): 1–12. https://doi.org/10.1038/sdata.2015.42.

Mann, H. 1945. "Nonparametic Test Against Trend." *Econometrica* 13: 245–59.

McCall, K.2013. "Managing Raindrops in the Lake Tahoe Basin: Projected Increase in Kinetic Energy Impact Around Fallen Leaf Lake as Climate Warms Snowfall into Rain." MS thesis, Humboldt State University, Arcata, CA, 36 pp.

Moussouni, A., L. Mouzai, and M. Bouhadef. 2014. "The Effect of Raindrop Kinetic Energy on Soil Erodibility." *International Journal of Environmental and Ecological Engineering* 8 (12): 879–83.

Natural Resource Conservation Service. 2017. "Snow Telemetry (SNOTEL) and Snow Course Data and Products." https://www.wcc.nrcs.usda.gov/snow.

Pierce, D., D. Cayan, T. Das, E. Maurer, N. Miller, Y. Bao, M. Kanamitsu et al. 2013. "The Key Role of Heavy Precipitation Events in Climate Model Disagreements of Future Annual Precipitation Changes in California." *Journal of Climate* 26 (16): 5879–96.

Pierce, D., D. Cayan, and B. Thrasher. 2014. "Statistical Downscaling Using Localized Constructed Analogs (LOCA)." *Journal of Hydrometeorology* 15: 2558–85.

Pierce, D., S. Cayan, E. Maurer, J. Abatzoglou, and K. Hegewisch. 2015. "Improved Bias Correction Techniques for Hydrologic Simulation of Climate Change." *Journal of Hydrometeorology* 16: 2421–42.

Pierce, D., J. Kalansky, and D. Cayan. 2018. "Climate, Drought, and Sea Level Rise Scenarios for California's Fourth Climate Change Assessment." California Energy Commission, Publication number: CCCA4-CEC-2018-014, 78 pp.

Polade, S., A. Gershunov, D. Cayan, M. Dettinger, and D. Pierce. 2017. "Precipitation in a Warming World: Assessing Projected Hydro-Climate Changes in California and Other Mediterranean Climate Regions." *Scientific Reports* 7 (1). https://doi.org/10.1038/s41598-017-11285-y.

Prein, A., R. Rasmussen, K. Ikeda, C. Liu, M. Clark, and G. Holland. 2016. "The Future Intensification of Hourly Precipitation Extremes." *Nature Climate Change* 7: 48–52. https://doi.org/10.1038/NCLIMATE3168.

Pupacko, A. 1993. "Variations in Northern Sierra Nevada Streamflow, Implications of Climate Change." *Water Resources Bulletin* 29: 283–90.

R Core Team. 2017. *R: A Language and Environment for Statistical Computing*. Vienna, Austria: R Foundation for Statistical Computing.

Roberts, D., and J. Reuter. 2007. "Lake Tahoe Total Maximum Daily Load Technical Report California and Nevada." In California Regional Water Quality Control Board and Nevada Division of Environmental Protection, South Lake Tahoe, CA and Carson City, NV, 341 pp.

Rogers, J. 1974. *Soil Survey of the Tahoe Basin Area, California and Nevada*. Washington, D.C.: USDA Soil Conservation Service.

Sahoo, G., S. Schladow, J. Reuter, R. Coats, M. Dettinger, J. Riverson, B. Wolfe, and M. Costa-Cabral. 2013. "The Response of Lake Tahoe to Climate Change." *Climatic Change* 116: 71–95.

Sakamoto, Y., M. Ishiguro, and G. Kitagawa. 1986. *Akaike Information Criterion Statistics*. Dordrecht, Holland: Reidel.

Schuster, S., and M. Grismer. 2004. "Evaluation of Water Quality Projects in the Lake Tahoe Basin." *Environmental Monitoring and Assessment* 90: 225–42.

Sempere-Torres, D.1992. "Quantification of Soil Detachment by Raindrop Impact: Performance of Classical Formulae of Kinetic Energy in Mediterranean Storms." In *Erosion and Sediment Transport Monitoring Programmes in River Basins*, edited by J. Bogen, D.E. Walling, and T.J. Day, 115–24. Oslo, Norway: IAHS.

Van Dijk, A., L. Bruijnzeel, and C. Roswill.2002. "Rainfall Intensity-Kinetic Energy Relationships: A Critical Literature Appraisal." *Journal of Hydrology* 261 (1-4): 1–23.

Wahl, K.L.1992. "Evaluation of Trends in Runoff in the Western United States." In *Managing Water Resources during Global Change. 28th Annual Conference & Symposium*, edited by R. Herrmann, 701–10. Reno, NV: American Water Resources Association.

Wischmeier, W.H., and D.D. Smith. 1958. "Rainfall Energy and Its Relationship to Soil Loss." *Transactions, American Geophysical Union* 39: 285–91.